Proceedings of the ASME 2010 3rd Joint US-European Fluids Engineering Summer Meeting and 8th International Conference on Nanochannels, Microchannels, and Minichannels
FEDSM-ICNMM2010
August 1-5, 2010, Montreal, Canada

FEDSM-ICNMM2010-31026

REYNOLDS NUMBER DEPENDENCE FOR LAMINAR FLOW LOSS COEFFICIENTS IN TEE AND WYE JUNCTIONS

Chris C. Kiser
Department of Engineering and Physics
University of Central Oklahoma
100 N. Univ. Dr.
Edmond, Oklahoma 73034
USA
405-974-5473, 405-974-3812, ckiser@uco.edu

Tim A. Handy
Department of Scientific Computing
Florida State University
400 Dirac Science Library
Tallahassee, Florida 32306-4120
USA
850-644-1010, tah09e@fsu.edu

Evan C. Lemley
Department of Engineering and Physics
University of Central Oklahoma
100 N. Univ. Dr.
Edmond, Oklahoma 73034
USA
405-974-5473, 405-974-3812,
elemley@uco.edu

Dimitrios V. Papavassiliou
School of Chemical, Biological and Materials Engineering
University of Oklahoma
100 East Boyd, SEC T-335
Norman, Oklahoma 73019
USA
405-325-5811, 405-325-5813,
dvpapava@ou.edu

Henry J. Neeman
OU Supercomputing Center for Education & Research
University of Oklahoma
Stephenson Research & Technology Center
SRTC/HPC, 101 David L. Boren Blvd.,
Norman Oklahoma 73019
USA
405-325-5386, 405-325-3442,
hneeman@ou.edu

ABSTRACT

In fluid flow piping systems, tee and wye junctions are commonly encountered and the study of flow through them has been well documented. Most of these studies have focused on flow characterized as turbulent for which there are nearly constant losses in pressure and kinetic energy in the junctions. Laminar flow has received much less attention since it is not frequently observed in macro scale piping systems where pipe diameters are measured in centimeters. The recent increase in use of micro scale flow devices calls for more research into laminar flow behavior that dictates the design and operation of these devices.

This paper documents results from computational fluid dynamics (CFD) simulations of flow in planar tee and wye junctions. The junctions studied consisted of circular pipes with two outlets and one inlet. The angles between the tee and wye junctions were fixed to 180 and 60 degrees, respectively. The inlet pipe diameter was fixed at 50 microns and the outlet pipe diameters were chosen to satisfy the continuity equation constrained to have equal velocities in all pipes. The lengths of the inlet and outlet pipes were varied to achieve fully developed flow within the junction. Following a grid resolution study performed on a sample tee junction, a generalized algorithm was designed and implemented to create three-dimensional models of these junctions subject to the former conditions.

In the CFD simulations, Reynolds number was varied in the laminar characterized region between 1 and 2000. The

simulations calculated static pressure and velocity magnitude values for a number of planes intersecting the junctions along the inlet and outlet pipes. From these values, pressure and kinetic energy gradients were calculated to estimate the static pressure and kinetic energy at the inlet and outlet pipes of each junction. Finally, these inlet and outlet values were used to calculate the stagnation pressure loss coefficient, which reflects dimensionless losses of pressure and kinetic energy for the junction. These coefficients ranged from 1 to 300 for the tee junction and 1 to 400 for the wye junction over the specified range of Reynolds number. The values were inversely proportional to Reynolds number and curve fits were provided for valid ranges.

INTRODUCTION

Flow devices and piping systems are being manufactured on the micro scale in increasing numbers as better processes are developed to produce them. Many flow devices such as valves, sensors, pumps, and electronic components used to make transistors in computer chips are available in the micrometer range [8-10]. These devices are often comprised of micrometer sized pipes and channels that bend and split into wyes or tees within a plane. One example of these are the series connected micro channels described by Lee et al [8]. Nature also produces micro scale materials known as porous media which are made up of interconnected pores [1-7]. These pores may be treated as a system of interconnected pipes which regularly form tee and wye junctions.

The commonality with these micro scale devices and systems is the characterization of their flow as laminar in many cases. Flow is characterized by the dimensionless parameter known as Reynolds number shown below (see next section for full parameter descriptions).

$$Re_d = \frac{Ud}{\nu} \tag{1}$$

A Reynolds number less than or equal to 2000 is considered to be laminar by most standards. Now if we were to consider two piping systems with different values of d and the same values U and ν, then Re_d becomes proportional to d. This parameter is the representative diameter of the device or system. If the diameters of these systems were chosen to be on the order of one centimeter and one micrometer, respectively, then Re_d of the latter system would be 1000 times smaller than the former. Therefore, it is easy to see why laminar flow is frequently observed in a microscale system that would not otherwise be seen in a larger system.

Tee and wye shaped junctions have been studied experimentally using turbulent flow (Re_d > 10000) [11-16]. These experiments determined the losses in pressure and velocity across two branches of a junction. Laminar flow pressure and velocity losses have also been determined experimentally for pipe fittings (e.g. elbows, expansions, contractions, and valves) by Edwards et al. [17] and for tees by Jamison et al. [18]. In both cases, the losses were transformed into a dimensionless loss coefficient and plotted as a function of Reynolds numbers.

Our goal was to determine a dimensionless loss coefficient as a function of Re_d over the range of 1 to 2000. The data could then be curve fitted using nonlinear regression and compared to laminar loss coefficients obtained by Jamison. A companion paper by Lemley et. al. [20] also describes an experimental system that is being used to determine loss coefficients in milli-scale junctions similar to those in this paper.

NOMENCLATURE

A_i	cross sectional area of pipe i (m²)
d_1, d_2, d_3	pipe diameters, as seen on Fig. 1 (m)
f_i	flow fraction (-)
K_i	stagnation loss coefficient in outlet pipe i (-)
L_i	length of pipe (m)
$\dot{m}_i$	mass flow rate in pipe i (kg/s)
p_i	pressure at location i (Pa)
Q_i	volumetric flow rate in pipe i (m³/s)
Re_d	Reynolds number based on pipe diameter and mean velocity (-)
u_i	velocity (m/s)
U	mean velocity in pipe (m/s)
x, y	spatial coordinates

Greek characters

θ	angle between the outlet pipes (°)
ρ	density (kg/m³)
ν	kinematic viscosity (m²/s)

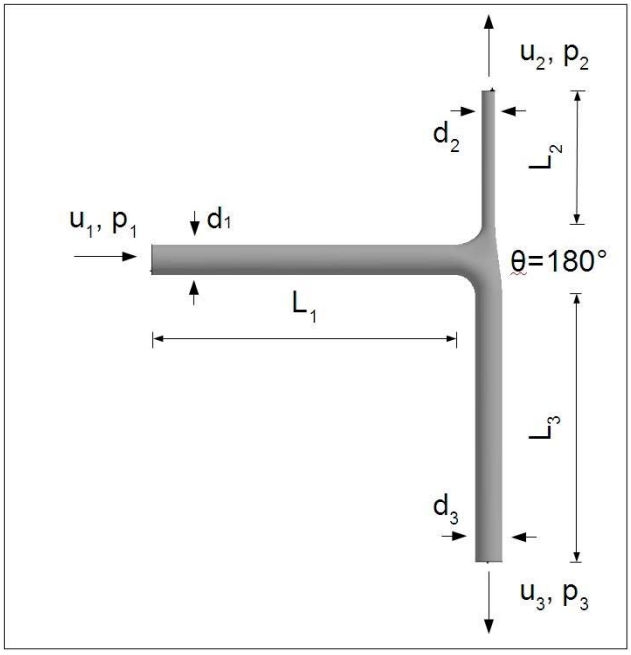

FIGURE 1. Sample tee junction with labeled parameters.

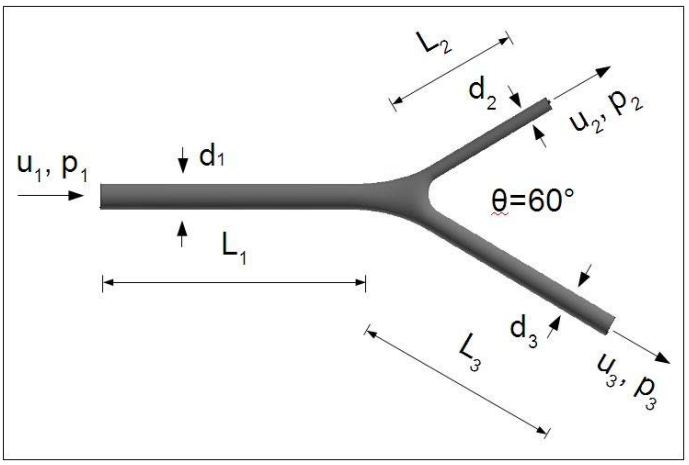

FIGURE 2. Sample wye junction with labeled parameters.

PROBLEM DESCRIPTION

The problem to be solved may be seen in Figs. 1 and 2. These figures are representative examples of the tee and wye junctions used in this study. From these junctions we would like to determine the laminar stagnation pressure loss coefficient and its dependence on Reynolds number. The stagnation pressure loss coefficient for an outlet pipe is defined as

$$K_i = \frac{\left[\left(\frac{p_1}{\rho} + \frac{u_1^2}{2}\right) - \left(\frac{p_i}{\rho} + \frac{u_i^2}{2}\right)\right]}{\frac{u_1^2}{2}} \tag{2}$$

The 1 and *i* subscripts refer to the inlet pipe and an outlet pipe, respectively. The process used to determine this loss coefficient requires the creation of a specific tee or wye geometry, meshing of that geometry, and simulation of the meshed geometry using a CFD software. These steps are elaborated on in the next section.

SOLUTION METHODOLOGY

As mentioned in the previous section, the process of determining K_i for the two outlet pipes requires many steps. Each of these steps requires a different software packages. A large amount of computer code, written in C++ and VBA among others, was used to automate these steps and calculate the values of K_i for several configurations of the tee and wyes in a shorter time span.

The first step was to create the geometry of either the tee or the wye junction. A computer automated design or CAD software package was used to create an arbitrary base junction with allowable values of θ between 30 and 180 degrees and a large range of allowable values for outlet pipe diameter ratios d_2/d_1 and d_3/d_1. Fig. 3 is an example of a tee base junction with different values of diameter ratios.

FIGURE 3. Tee base junction created using CAD software.

The diameter ratios were determined by constraining the continuity equation to have equal velocities at the inlet and both outlet pipes. The continuity equation is defined by

$$\dot{m}_1 = \dot{m}_2 + \dot{m}_3 \tag{3}$$

where

$$\dot{m}_i = \rho u_i A_i$$

and

$$Q_i = u_i A_i$$

The fluid used in the simulations was water at room temperature which is incompressible (constant ρ). This leads to

$$Q_1 = Q_2 + Q_3$$

Dividing this result by Q_1 leads to Eq. 3 expressed in terms of flow fractions

$$1 = f_2 + f_3 \tag{4}$$

where

$$f_i = \frac{Q_i}{Q_1} = \frac{A_i u_i}{A_1 u_1} = \left(\frac{D_i}{D_1}\right)^2 \frac{u_i}{u_1}$$

Substituting in our constraint $u_i=u_1$ and rearranging gives the diameter ratio as

$$\left(\frac{D_i}{D_1}\right) = \sqrt{f_i} \tag{5}$$

Therefore, if we specify a value of f_2 or f_3, the corresponding diameter ratio can be calculated using Eq. 5 and Eqs. 4 and 5 can be used to calculate the remaining flow fraction and diameter ratio, respectively. In this study, f_2 was specified for values of 0.1, 0.2, 0.3, 0.4 and 0.5.

The next step was to import the base junction into GAMBIT to create the final geometry. This involves adding cylinders to the geometry in Fig. 3. The reason for this is that

in order for the flow in the inlet and outlet pipes to be considered fully developed (constant velocity profile), the entrance lengths must satisfy the modified entrance length equation suggested by Lemley et. al [19] and expressed as

$$L_e = 0.1 Re_d \; d \tag{6}$$

Each length L_1, L_2, and L_3 was calculated using Re_d and the corresponding diameter d_1, d_2, and d_3. The three cylinders with lengths given by Eq. 3 are then attached to the base junction to create a final geometry (e.g. Fig. 1).

Once the final geometry was generated, it needed to be meshed for CFD simulations. The meshing process involves dividing the geometry into volume elements. Fig. 4 shows a meshed tee junction using the base junction seen in Fig. 3. The cylinders attached to the base junction were meshed using nodes along the axis of the cylinder and around the circumference of the cylinder. Fig. 5 shows the spacing of the circumferential and axial nodes used in the mesh in Fig. 4. Varying the number of circumferential (face) nodes and axial (edge) nodes determines how coarse or fine the meshed junction becomes. The number of face and edge nodes also has an impact on the resulting loss coefficients K_2 and K_3. For this reason a grid resolution study was needed.

The grid resolution was performed on a tee junction with the following geometry: inlet diameter of 50μm, outlet diameter ratios both set to unity, flow fractions in outlet pipe two set to 0.25 and 0.5, and Reynolds numbers of 10, 100, and 1000. The reason for using multiple values of f_2 and Re_d was to determine if the grid resolution had any dependence on these quantities. Grid resolution was determined by first using a constant number of edge nodes and varying the face nodes. Next, the number of face nodes was held constant while the number of edge nodes was varied. In each case, the grid resolution was refined from coarse to fine by increasing either the number of face or edge nodes. The six resulting loss coefficients were obtained for each combination of edge nodes and face nodes. These coefficients were compared using percent error to the finest grid resolution simulated with either a fixed number of edge nodes or a fixed number of face nodes. The criterion for convergence was selected such that the percent error was within 10%. Table 1 shows the loss coefficients for a flow fraction of 0.5, 25 edge nodes, and varying face nodes. Table 2 shows the loss coefficients for a flow fraction of 0.5, 40 face nodes, and varying edge nodes.

The grid resolution study revealed that comparing the grid combination with 120 face nodes and 25 edge nodes to the grid combination with 135 face nodes and 25 edge nodes resulted in the convergence criterion being met. The latter combination was used as the finest available resolution to which all other combinations with 25 edge nodes were compared. The study also revealed that comparing the grid combination with 120 face nodes and 100 edge nodes to the grid combination with 120 face nodes and 250 edge nodes also resulted in the convergence criterion being met. The latter combination here was used as the finest available resolution to which all other combinations with 120 face nodes were compared. Therefore, the grid combination containing 120 face nodes and 100 edge nodes was selected as sufficient for our simulations. This grid combination contains 731691 volume elements. Finally, the study showed no dependence of the convergence criterion being met by changing f_2 and Re_d.

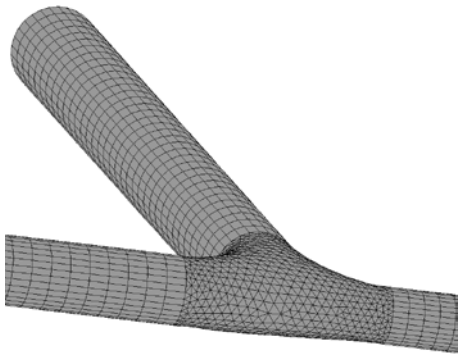

FIGURE 4. Meshed tee generated in GAMBIT using the base junction shown in Fig. 3.

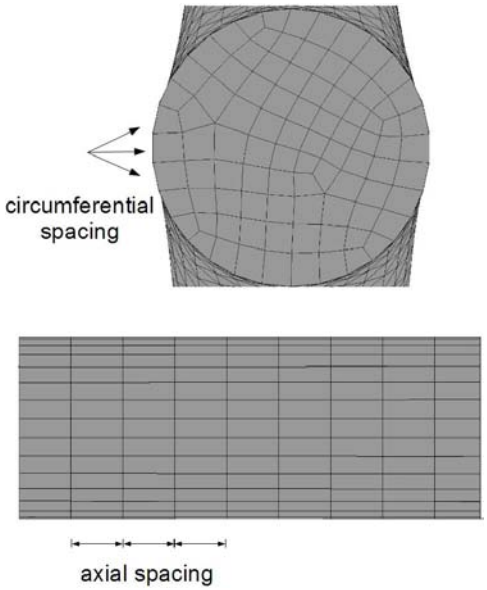

FIGURE 5. Close up of mesh tee showing circumferential and axial spacing of nodes on the junction face and edge, respectively.

TABLE 1. Loss coefficients for fixed flow fraction and number of edge nodes of 0.5 and 25, respectively.

Number of Face Nodes	Reynolds Number		
	10	100	1000
15	6.55	1.14	1.08
30	6.76	0.99	0.79
45	6.95	0.90	0.58
60	8.07	0.73	0.73
75	8.24	0.71	0.82
90	8.91	0.67	0.66
105	9.75	0.76	0.64
120	10.73	0.85	0.49
135	10.98	0.88	0.49

TABLE 2. Loss coefficients for fixed flow fraction and number of face nodes of 0.5 and 120, respectively.

Number of Edge Nodes	Reynolds Number		
	10	100	1000
25	10.73	0.85	0.49
50	9.99	0.74	0.34
75	10.59	0.83	0.44
100	10.24	0.76	0.37
250	10.53	0.82	0.40

With the geometry created and the appropriate mesh applied, the final step was to export the meshed geometry to a CFD software package for simulation. The software chosen for this study was FLUENT. FLUENT employs a finite volume method to solve the integral Navier-Stokes equations for steady state flow conditions in three dimensions. FLUENT uses a solver with a SIMPLEC algorithm for pressure-velocity coupling, a second order upwind scheme for momentum discretization, and a convergence criterion of 0.001%. The boundary conditions used in FLUENT were the velocity inlet and outflow boundary. The velocity inlet boundary condition assumes a uniform velocity profile at the inlet pipe which corresponds to the chosen Re_d. The outflow boundary condition assumes that the velocity profile is fully developed at the two outlet pipes of the junction. The fully developed velocity profile was satisfied for the inlet and outlet pipes of each junction by using Eq. 6 to calculate the entrance lengths of the attached cylinders in GAMBIT. The outflow boundary condition also allowed us to set the flow fractions in outlet pipes to the desired values. Circular planes are defined along the axis of each cylinder which intersect the cylinder and divide it into sections. Velocity and pressure values obtained from the Navier-Stokes equations by the solver are specified at the center of each of these planes where the flow is fully developed. From these values, the pressure and velocity gradients along each cylinder were calculated. With the pressures and velocities known at the inlet and outlet pipes of the base junction itself, one can substitute these values into Eq. 2 to obtain K_2 and K_3.

RESULTS

The loss coefficients were determined for five tee geometries and five wye geometries. The geometries included a range of diameter ratios between 0.316 and 0.949 with corresponding flow fractions between 0.1 and 0.9. Fifteen values of Reynolds number were specified for the tee junction and ten values were specified for the wye junction. These values were selected so that they would be evenly spaced on a log-log plot of K vs Re_d. The resulting plots are shown in Figs. 6 and 7. From these plots one can see that the K is inversely proportional to Re_d over the range of 1 to about 300 at which point K becomes nearly constant. One may also see that K decreases as f increases. This is due to the outlet diameter's dependence on f (Eq. 5).

Curve fits were then generated to fit the data. A nonlinear regression technique was used to determine the proportionality constant between K and Re_d. Table 1 shows the proportionality constant, labeled C, for the nine flow fractions in each junction. These fits are for the general equation

$$K = \frac{C}{Re_d} \tag{7}$$

and are only value over the linear section of the observed data. The valid range of Re_d for the curve fits was chosen to be from 1 to 100. Within this range the maximum percent difference between the predicted and simulated values of K for any flow fraction is estimated at 30%. The largest values of K were obtained for a Re_d of 1 and were equal to 287.8 for the tee and 395.9 for the wye. The smallest value of K was obtained as a constant value for $Re_d > 800$ and was slightly above 1 for both the tee and the wye.

A comparison was also made between the laminar loss coefficients obtain by our simulations and those obtained by Jamison et. al. [18] for a tee shaped junction. This comparison is shown in Fig. 8. The values obtained by Jamison are just over an order of magnitude greater than our simulated values. There are several differences between the two tee geometries, shown in Fig. 8, which are likely the cause of the difference in loss coefficient values obtained. Nevertheless, the values compared show good qualitative agreement.

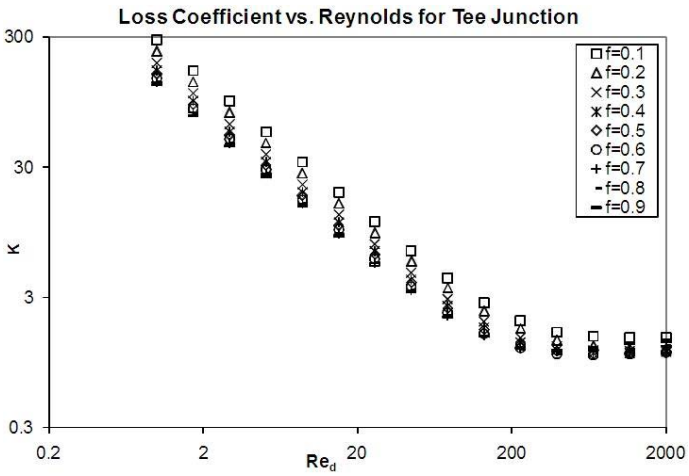

FIGURE 6. Loss coefficient vs Reynolds number for various flow fractions in a tee.

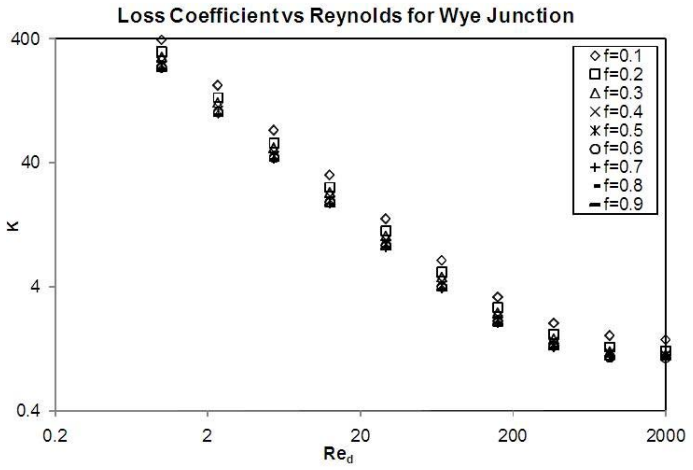

FIGURE 7. Loss coefficient vs Reynolds number for various flow fractions in a wye with θ=60°.

TABLE 3. Proportionality constants for various flow fractions.

Tee		Wye	
f	C	f	C
0.1	287.8	0.1	395.9
0.2	234.8	0.2	314.6
0.3	193.0	0.3	286.9
0.4	167.7	0.4	263.3
0.5	157.8	0.5	247.5
0.6	146.8	0.6	239.7
0.7	136.6	0.7	233.8
0.8	135.8	0.8	226.2
0.9	130.4	0.9	225.3

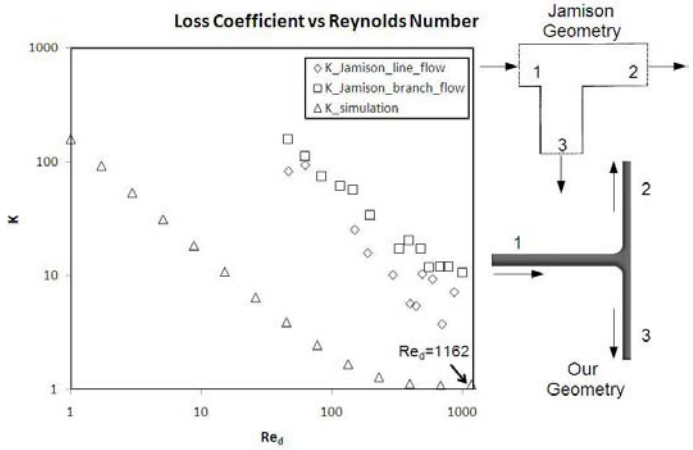

FIGURE 8. Loss coefficient vs Reynolds number comparison to experimental data.

CONCLUSIONS

The stagnation pressure coefficient was calculated for a range of Reynolds numbers between 1 and 2000 for tee and wye junctions having a angle ϑ of 180° and 60°, respectively. Ten junctions (five tee and five wye) were created using flow fractions specified between 0.1 and 0.9 with the corresponding diameter ratios calculated using Eq. 5. The resulting data showed an inversely proportional relationship between Re_d and K in all junctions. Curve fits were calculated to fit the linear sections of the data. The data was compared and has a good qualitative agreement with that of Jamison et al. [18].

ACKNOWLEDGMENTS

The Office of Research and Grants at the University of Central Oklahoma is acknowledged for support of this research. The Donors of The Petroleum Research Fund, administered by the American Chemical Society, are also be acknowledged for support of this research through grant PRF# 47193-B9. The National Science Foundation EPSCoR Research Opportunity Award Program is acknowledged in partial support of this research.

REFERENCES

1. Lao, H-W, Neeman, H.J., and Papavassiliou, D.V., 2004, "A Pore Network Model for the Calculation of Non-Darcy Flow Coefficients in Fluid Flow through Porous Media," Chem. Eng. Com., **191**(10), pp. 1285-1322.
2. Lin C.-Y. and J.C. Slattery, 1982, "Three-Dimensional, Randomized, Network Model for Two-Phase Flow Through Porous Media," AIChE J., **28**(2), pp. 311-324.
3. Dias, M.M. and Payatakes, A.C., 1986, "Network Models for Two-Phase Flow in Porous Media. Part 1. Immiscible Microdisplacement of Non-Wetting Fluids," J. Fluid Mech., **164**, pp. 305-336.
4. Rajaram, H., Ferrand, L.A., and M.A. Celia, 1997, "Prediction of Relative Permeabilities for Unconsolidated Soils using Pore-scale Network," Water Resources Research, **3**(1), pp. 43-52.
5. Dahle, H.K., and M.A. Celia, 1999, "A Dynamic Network Model for Two-Phase Immiscible Flow," Computational Geosciences, **3**, pp. 1-22.
6. Thauvin, F., and K.K. Mohanty, 1998, "Network Modeling of Non-Darcy Flow Through Porous Media," Transport in Porous Media, **31**, pp. 19-37.
7. Lemley, E.C., Papavassiliou, D.V., and H.J. Neeman, 2007, "Non-Darcy Flow Pore Network Simulation: Development and Validation of a 3D Model," *Proceedings of FEDSM2007*, 5th Joint ASME/JSME Fluids Engineering Conference, paper FEDSM2007-37278.
8. Lee, W.Y., Wong, M., and Zohar, Y., 2002, "Microchannels in Series Connected Via a Contraction/expansion Section", J. Fluid Mech., **459**, pp.187-206.
9. Graveson, P., Branebjerg, J., and Jensen, O.S., 1993, "Microfluidics a Review," J. Micromech. Microeng., **3**, pp.168-182.
10. Judy, J., Maynes, D., and Webb, B.W., 2002, "Characterization of Frictional Pressure Drop for Liquid Flows Through Microchannels," Intl. J. Heat Mass Trans., **45**, pp.3477-3489.

11. Basset, M.D., Winterbone, D.E., and Pearson, R.J., 2001, "Calculation of Steady Flow Pressure Loss Coefficients for Pipe Junctions," Proc. Instn. Mech. Engrs., Part C, Journal of Mechanical Engineering Science, **215** (8), pp. 861-881.
12. W.H. Hager, 1984, "An Approximate Treatment of Flow in Branches and Bends," Proc. Instn. Mech. Engrs., Part C, Journal of Mechanical Engineering Science, **198**(4) pp. 63-9.
13. Blaisdell, F.W., and Manson, P.W., 1967, "Energy loss at pipe junctions," J. Irrig. and Drainage Div., ASCE, **93**(IR3), pp. 59-78.
14. Schohl, G.A., 2003, "Modeling of Tees and Manifolds in Networks," *Proceedings of the 4th ASME/JSME Joint Fluids Engineering Conference*, **2**, Part D, pp. 2779-2786.
15. Bassett, M.D., Pearson, R.J., and Winterbone, D.E., 1998, "Estimation of Steady Flow Loss Cofficients for Pulse Converter Junctions in Exhaust Manifolds," *IMechE Sixth International Conference on Turbocharging and Air Management Systems*, IMechE HQ, London, UK, **C554/002**, pp.209-218.
16. Ruus, E., 1970, "Head Losses in Wyes and Manifolds," J. Hyd. Div., ASCE, **96**(HY3), 593-608.
17. Edwards, M.F., Jadallah, M.S.M., and Smith, R., 1985, "Head Losses in Pipe Fittings at Low Reynolds Numbers," Chem. Engr. Res. Des., **63**(1), pp. 43-50.
18. Jamison, Donald K., and Villemonte, James R., 1971, "Junction Losses in Laminar and Transitional Flows," Journal of the Hydraulics Division, **97**(7) pp. 1045-1063.
19. Lemley, E.C. et. al., 2009, "Laminar Entrance Length In Microtubes," *Proceedings of FEDSM2009,* 2009 ASME Fluids Engineering Conference, paper FEDSM2009-78532.
20. Lemley, E.C. et. al., 2010, "Milli-Scale Junction Flow Experiments," *Proceedings of FEDSM2010-ICNMM2010,* ASME 2010 3rd Joint US-European Fluids Engineering Summer Meeting and 8th International Conference on Nanochannels, Microchannels, and Minichannels, paper FEDSM2010-ICNMM2010-30123.